Transverse Tensile Strength Prediction of Thermosetting Composites

SAGAR P. SHAH and MARIANNA MAIARU

ABSTRACT

The transverse tensile strength of composites is susceptible to size effects. Therefore, it is paramount to develop length-scale specific physical test procedures to validate computational models that estimate the transverse composite response using micromechanics. To this end, a computational process modeling and virtual mechanical testing framework are presented in this study to predict the transverse response of composite microstructures subjected to processing conditions. Informed by a comprehensive material dataset, the numerical model is shown to reliably predict the process-induced residual stress generation in composite microstructures and accurately evaluate its influence on their transverse strength prediction. A novel procedure to fabricate thin composite laminates from a single ply of carbon fibers and characterize their transverse tensile response is presented to validate the numerical model. The results show excellent agreement with the virtual test predictions. This study highlights the importance of length-scale specific testing to minimize the influence of size effect on the transverse composite strength.

S. P. Shah, M. Maiaru, University of Massachusetts Lowell, Lowell, MA, USA 01854

INTRODUCTION

The field of computational materials engineering (CME) has seen rapid growth over the past few decades. Advances in high-performance computing, novel physics-based constitutive modeling, and new material characterization methods have propelled composite design and development, where existing material and structural designs can be improved and better-performing configurations can be designed, tested, and optimized computationally before they are actually manufactured [1]–[3]. However, there is a strong need for computationally light, efficient techniques that can accurately predict the multiscale composite response and estimate allowables to fully realize the potential of CME and replace the costly, time-consuming physical testing [2]–[4].

Constitutive modeling of failure in composites is fundamentally challenging due to their complex failure mechanisms that depend on the loading direction as well as the length scale considered [4], [5]. Several multiscale modeling strategies have been reported that can predict composite responses at different length scales [1], [3]–[11]. These strategies typically perform nano and microscale analyses to predict the microscale response of composites subjected to processing conditions and mechanical loads. The computed properties are then homogenized and empirically passed on to higher length scales to evaluate part performance and define allowables. While such model strategies are sound and widely accepted, an aspect often overlooked is the scaling of the mechanical properties between length scales. The size effect is typically observed in quasi-brittle material failure such as polymer matrix composites (PMCs) where the composite strength changes with the size of the specimen tested [12]–[16]. The matrix-dominated transverse tensile strength is particularly susceptible to size effects as has been reported in [12], [13], [15]. Ignoring the scaling of strength properties can lead to erroneous estimations of allowables. Nevertheless, capturing the size effect is extremely challenging due to the complex micro-/mesostructure that characterizes the composites at each length scale [14]. Thus, to ensure that the material properties predicted at a particular length scale and subsequently passed on to higher length scales are accurate, length scale-specific testing and validation procedures need to be established.

Although mechanical testing of composite laminates at mesoscale and higher is well established [7], [8], [12]–[18], microscale testing to predict transverse composite response remains largely unexplored due to the extremely complex and challenging nature of the tests needed. Consequently, coupon-level testing of stacked laminates (> 3 mm) is typically carried out to validate microscale numerical models (< 1 mm) [7], [19]. In addition to the size effect, coupon-level test specimens exhibit failure modes, such as inter-ply delamination, that may not be fully represented by numerical microscale models [8], [20]. To have a meaningful experimental validation of the numerical model, the length scales of the numerical simulations and the experiments must be comparable. Thus, there is a pressing need to develop experimental techniques to characterize composite responses at lower length scales to facilitate exploration, characterization, verification, and validation of constitutive material models as highlighted in NASA's Vision 2040 [2]. Only recently, Flores et al. [21] designed an experiment to test composite micropillars in transverse compression and observe micromechanical failure. Their pioneering work provided valuable insight into microstructural instabilities, effects of nanovoids, interfacial debonding, and matrix

cracking under transverse compressive loads while highlighting critical challenges that must be overcome to standardize such tests. To date, tests of such nature for transverse tension are lacking in the literature.

The objective of this work is to address the prediction of transverse tensile strength of PMCs using micromechanics. First, a robust computational process modeling framework is presented to allow the prediction of residual stresses in composite microstructures. The processed microstructures are then virtually tested under transverse tensile mechanical loads to predict the transverse composite response. The transverse composite stiffness and strength predictions from the virtual analysis are validated against physical testing of thin composite laminates (< 1 mm). A novel procedure to fabricate and test composite laminates from a single carbon fiber ply is presented. Size effect on transverse strength is discussed and the use of thin laminates for validation is justified.

METHODOLOGY

Materials

Unidirectional (UD) carbon fiber-reinforced polymer (CFRP) composite laminates, manufactured by infusing IM7 carbon fibers with an epoxy resin commercially sold as EPIKOTE™ Resin MGS™ RIMR 135 with EPIKURE™ Curing Agent MGS™ RIMH 1366 (henceforth referred to as RIM R135-H1366), were tested under transverse tension for their transverse strength characterization. For experimental procedures, composite laminates were fabricated from a single ply of IM7 carbon fiber to achieve a very thin laminate. The carbon fiber plies were supplied by Fibre Glast Developments Corp. while the RIM R135-H1366 rein system was supplied by Hexion Inc.

Computational Micromechanics

Computational process modeling and virtual mechanical testing of composite microstructures were carried out in commercial finite element (FE) software Abaqus. The details of representative volume element (RVE) generation, process modeling procedure, and virtual mechanical testing of the processed RVEs are discussed in the following sections.

RVE GENERATION

The thermo-mechanical response of the CFRP composites was determined by analyzing their microstructures through computational micromechanics. Here, the numerical representations of the composite microstructures were modeled in Abaqus. A random RVE generator, developed by Stapleton et al. [22], was employed to generate RVEs comprising a random dispersion of IM7 carbon fibers in a RIM R135-H1366 epoxy matrix. An RVE size consisting of 50 fiber inclusions was chosen based on the statistical size-effect study performed by Shah et al. [23]. Informed by the experimentally determined fiber volume fraction of the composite laminates (see Experimental Methods), the RVEs were modeled with $v_f = 0.60$. Five distinct realizations of the RVEs with random fiber distribution, see Figure 1, were analyzed to account for statistical variations in the numerical predictions. Perfect bonding was

assumed between the constituent fibers and matrix. The IM7 carbon fibers were modeled as transversely isotropic solids, the thermo-mechanical properties for which can be found in [23], [24]. The matrix was modeled as an isotropic material. The evolution of the matrix thermo-mechanical properties with the degree of cure ϕ and temperature T during process modeling was defined by experimentally determined material-specific models described in [24]. Each RVE was meshed with C3D8T elements. Flat boundary conditions (FBCs) were chosen for both process modeling and virtual mechanical testing, as illustrated in Figure 2.

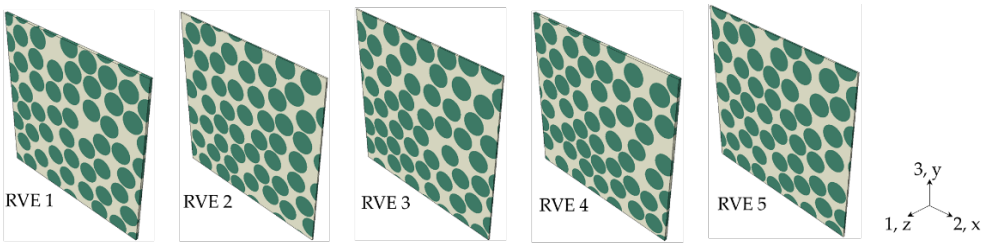

Figure 1: Five distinct realizations of a 50 fiber RVE with $v_f = 0.60$.

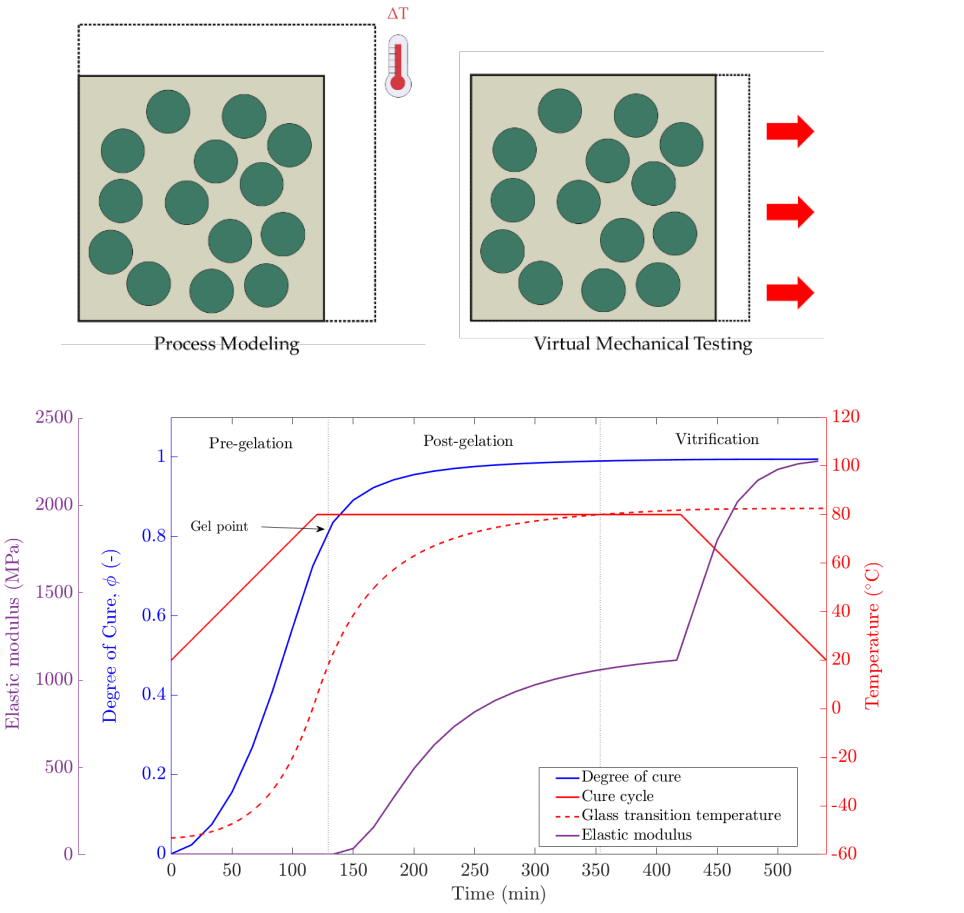

Figure 2: Illustrations of flat boundary conditions (FBCs) applied to the RVEs during process modeling and virtual mechanical testing analyses; evolution of the degree of cure ϕ, glass transition temperature T_g and elastic modulus E for a prescribed temperature cycle.

PROCESS MODELING AND RESIDUAL STRESS PREDICTION

The complete manufacturing of composites and the resultant residual stress generation in composite microstructures was captured by the process model developed by Shah et al [24]. A coupled temperature-displacement analysis was carried out in Abaqus/STANDARD with user-subroutines UMATHT and UMAT. The progression of cure, for a prescribed temperature profile, was defined by the Kamal-Sourour kinetic model [25],

$$\frac{\mathrm{d}\phi}{\mathrm{d}t} = \left[A_1 \exp\left(\frac{\Delta E_1}{RT^*}\right) + A_2 \exp\left(\frac{\Delta E_2}{RT^*}\right)\phi^m\right](1-\phi)^n \tag{1}$$

where kinetic constants $A_1 = 3.6 \times 10^9$ sec^{-1}, $A_2 = 0.01245$ sec^{-1}, $\Delta E_1 = 85.3$ kJ/mol, $\Delta E_2 = 11.1$ kJ/mol, $m = 0.4$, and $n = 1.5$ were experimentally determined as reported in [24]; R is the universal gas constant and T^* is the absolute temperature in degrees Kelvin. The kinetic model was simultaneously solved with a 3-dimensional Fourier heat transfer equation to predict the progression of cure and temperature distribution within the RVE. For a given cure state and temperature within the RVE, the instantaneous in-situ matrix properties were computed with the help of material-specific models reported in [24]. The development of the matrix glass transition temperature and elastic modulus with the degree of cure and temperature, based on the relations reported in [24], are graphically presented in Figure 2. The subsequent residual stress generation was modeled with an instantaneous linear elastic constitutive model

$$\sigma_i(t) = \left[C_{ij}(t)\right]\left[\epsilon_j^{total}(t) - \left(\epsilon_j^{th}(t) + \epsilon_j^{sh}(t)\right)\delta_j\right] \quad \text{where} \quad \begin{cases}\delta_j = 1 \text{ if } j = 1,2,3\\ \delta_j = 0 \text{ if } j > 3\end{cases} \tag{2}$$

where i and j are Voigt notation indices; $\epsilon_j^{total}(t)$, $\epsilon_j^{th}(t)$ and $\epsilon_j^{sh}(t)$ are the total, thermal and chemical shrinkage strains, respectively; $\left[C_{ij}(t)\right]$ is the stiffness matrix as a function of the time of cure; $\sigma_i(t)$ is the accumulated residual stress governed by the development of the in-situ matrix elastic modulus and the chemical and thermal strains experienced by the matrix. Here, the curing matrix was prescribed a constant strength and fracture toughness as reported in [23], [24].

VIRTUAL MECHANICAL TESTING

Following the process modeling analysis, each of the processed RVEs was subjected to transverse tensile mechanical loads to predict their transverse composite response, namely the transverse composite strength σ_{22}^{+} and stiffness E_{22}^{+}.

Failure in the matrix was modeled with a previously developed progressive damage model [23] based on the theory of crack band [26] and implemented in Abaqus/EXPLICIT with VUMAT user-subroutine. The maximum principal stress criterion was used to define failure initiation in the matrix. A traction-separation law, governed by the fracture energy, was used to define the post-peak softening behavior [23], [27]. The traction-separation law employed a normalized value of the fracture toughness G_{IC} to preserve mesh objectivity. A scalar damage factor was defined to

degrade the components of the compliance matrix of the damaged material. The numerical implementation details and matrix material properties can be found in [23].

Experimental Methods

SPECIMEN FABRICATION AND SPECIFICATION

Tensile testing of thin composite laminates was carried out as per ASTM D3039 [28]. The thin carbon fiber laminates were fabricated in-house using the vacuum-assisted resin transfer molding (VARTM) [20] approach as illustrated in Figure 3. Here, single plies of unidirectional IM7 carbon fibers were infused with epoxy at room temperature under a constant vacuum of 29 inches of Hg. To avoid dry patches/void formations and maximize resin retention, the infusion was performed perpendicular to the fiber direction. The infused panels were cured in a convection oven programmed to run the temperature profile shown in Figure 2 while under vacuum. The resulting panels were 450 mm × 300 mm in dimensions with an average thickness of 0.95 mm. Subsequently, rectangular test specimens of various sizes were cut out from different sections of the panel for fiber volume fraction determination and tensile test specimen preparation.

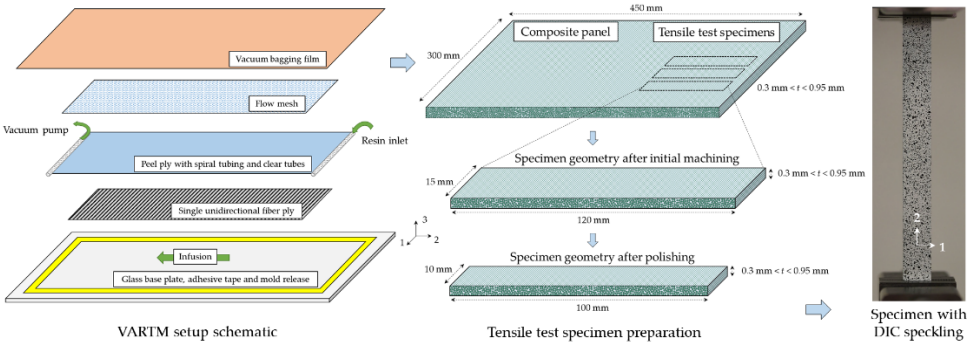

Figure 3: Schematic of the procedure to fabricate thin composite laminate through VARTM and prepare tensile test specimens.

Mass density measurements and thermo-gravimetric analyses (TGA) were performed to determine the fiber volume fraction. As per ASTM D792 [29], ten rectangular specimens (10 mm × 10 mm) were tested at room temperature for their mass density using a Sartorius Practum 313-1S precision balance equipped with a Sartorius YDK01 density measurement kit. Following that, the density measurement specimens were repurposed to determine the fiber mass fraction with a TA Instruments Discovery TGA per ASTM E1131 [30]. Before the test, the specimens were allowed to air-dry for 24 hours to dry off any moisture absorbed during the density measurement test. Then, the specimens were tested in the TGA where the initial mass of the specimen was measured, and the specimen was heated from room temperature to 750°C at a temperature rate of 15°C/min. During the test, the resin content burnt off, and the residue in the TGA crucible was regarded as the fiber content. Based on the combined density measurement and TGA data, the fiber volume fraction was determined as $v_f = 0.60$.

To prepare the tensile test specimens, rectangular specimens with 120 mm × 15 mm dimensions were cut out. The specimen dimensions were deliberately chosen larger

than the target dimensions of 100 mm × 10 mm to account for the material removed during polishing. The specimens were initially cut using a wet saw equipped with a diamond-tip blade. After initial machining, the specimens were lightly sanded with a coarse sandpaper (120-grit) on a Buehler MetaServ 250 waster polished to remove any surface scratches and fiber blowout from the machining. Subsequently, the specimen edges were incrementally fine-sanded (up to 3200-grit) to achieve a smooth and crack-free surface. Once the target specimen dimensions were achieved, the specimens were coated with a speckle pattern for 2D DIC strain measurement as shown in Figure 3.

TENSILE TEST PROCEDURE

Uniaxial quasi-static tension tests were carried out as per ASTM D3039 [28] to characterize the transverse composite response of thin laminates. A displacement-controlled test with a crosshead displacement rate of 2 mm/min was performed using an ElectroForce 3200 (TA Instruments) equipped with a 450 N load cell and heavy-duty tension grips to test the specimens. Prior to each test, the specimen width and thickness were measured at three different locations along the gage length. The average cross-sectional area along the gauge length was used to convert the force output data from the load cell to nominal stress.

The full-field strains of the deforming specimens were measured throughout the testing procedure with the 2D DIC technique [31]–[33] using a Canon EOS Rebel T3i camera. The NCorr software packing was utilized for DIC image processing [31], [32]. An in-house postprocessor program was developed in MATLAB to process and correlate the raw time-load-displacement data extracted from the tensile test apparatus with the strain data from NCorr analysis. The corrected strains from the postprocessor were matched with the nominal stress values to yield a stress versus strain plot. The transverse composite stiffness was defined as the slope of the linear region of this plot while the composite strength was defined as the maximum load sustained by the specimen prior to failure. The data from five good breaks along the gage length were assumed to comprise a good sample size per the ASTM D3039 standard [28].

RESULTS AND DISCUSSION

A computational process modeling framework was employed to predict the transverse tensile response of composite microstructures by subjecting randomly packed RVEs to virtual processing conditions and subsequently testing them under virtual transverse tensile loads. The transverse response in terms of the transverse stiffness and strength were extracted from their stress versus strain plots and compared with the corresponding values obtained from physical testing of thin composite laminates manufactured under the same processing conditions. An additional case of virtual mechanical testing was introduced where the RVEs were assumed to cure under "ideal" conditions resulting in zero residual stress generation at the end of processing. This allowed for the quantification of the effect of process-induced residual stresses on the transverse composite performance.

For the process modeling analysis, the RVEs were subjected to the temperature profile shown in Figure 2 during which the matrix material cured in-situ and experienced residual stress generation due to its elastic modulus development, chemical shrinkage strains, and thermal mismatch between the constituents. The contour plot of

the end-of-cure residual stresses (maximum principal) is shown for one representative microstructure in Figure 4. Residual stress generated during cure was predicted for all RVEs illustrated in Figure 1.

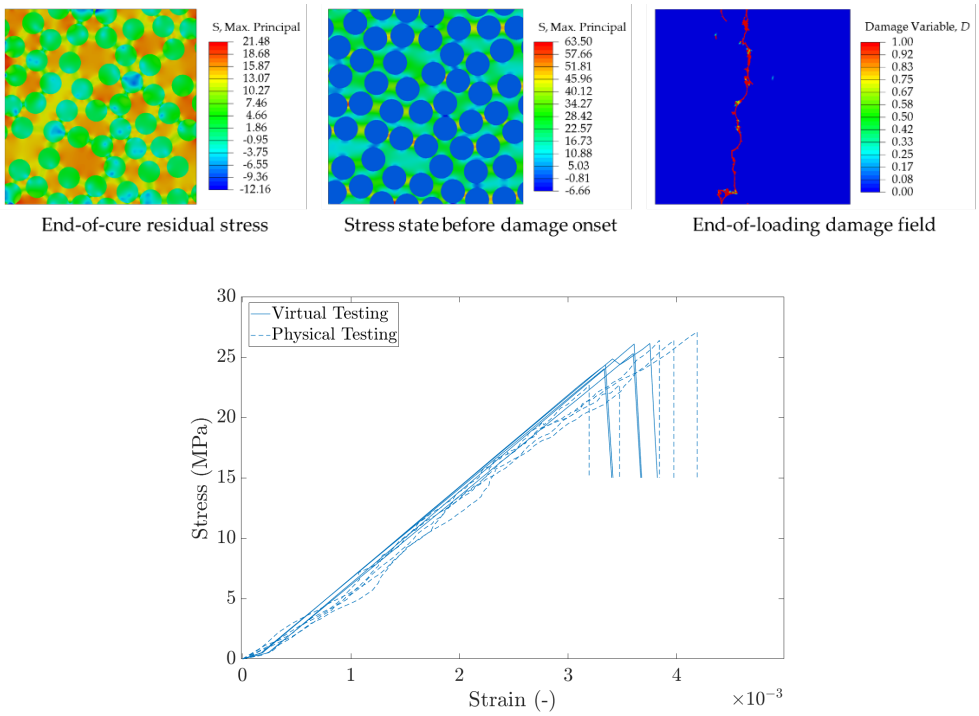

Figure 4: Contour plot of end-of-cure residual stresses (maximum principal) from process modeling analysis, maximum principal stresses before the onset of damage from virtual mechanical testing, and damage field in the RVE at the end of the virtual mechanical testing; the plot of nominal stress versus strain from virtual testing of RVEs with $v_f = 0.60$ and physical testing of thin laminates.

The processed RVEs were then subjected to virtual mechanical loads in the transverse direction to predict their transverse stiffness and strength. The stress versus strain plots of the five RVEs, presented in Figure 4, exhibit an initial linear elastic response which was followed by a drop in the stress. This drop was associated with damage initiation in the matrix when maximum principal stresses exceeded the matrix strength. The contour plot of the maximum principal stress before the onset of damage, shown in Figure 4, clearly highlights the regions of high stress concentrations where failure initiation was anticipated. The contour plot of the end-of-loading damage field, seen in Figure 4, also implies that failure is initiated in regions of dense fiber packing where stress is concentrated leading to local microcracking. These cracks eventually coalesced into a large crack resulting in a two-piece failure. The average transverse composite stiffness $E_{22}^{+} = 7503.18 \pm 89.3$ MPa (computed from the initial slope of the stress versus strain plot) and strength $\sigma_{22}^{+} = 25.17 \pm 0.86$ MPa (computed as the maximum stress before failure) for the five RVEs were obtained. Similar analyses were carried out for RVEs neglecting the effect of residual stress. These RVEs reported an average transverse composite stiffness $E_{22}^{+} = 7502.02 \pm 88.57$ MPa and strength $\sigma_{22}^{+} = 28.64 \pm 1.16$ MPa. Although no significant difference was reported in the transverse composite stiffness between the RVEs neglecting residual stresses and the process modeled RVEs, a significant change in the transverse strength was observed. In fact, the transverse composite strength was overestimated by 12.9% when the process-

induced residual stresses were ignored. Therefore, is was observed that process-induced residual stresses influence the transverse composite strength, and their effect must be considered during composite part design.

The nominal stress versus strains from DIC measurements for the quasi-static transverse tension testing of thin laminates is presented in Figure 4. As seen in Figure 4, the specimens manifest a fairly linear response leading to a macroscopic failure, which was defined as a large drop in the stress. Some initial non-linearity, observed in the specimen's response, was attributed to the specimens settling within the grips while the pre-failure non-linearity was attributed to the change in the specimen compliance on account of local microcracking. The corrected strains matched with the corresponding stresses yielded the transverse composite stiffness as $E_{22}^{+} = 7173.23 \pm 76.43$ MPa. The transverse composite strength $\sigma_{22}^{+} = 25.08 \pm 1.97$ MPa. A comparison with the numerical predictions obtained in the previous section showed excellent agreement. The numerical stiffness and strength predictions from the model were within 97% and 95% accuracy of those obtained from physical testing, respectively.

These results clearly show that accurate, physics-based modeling tools are critical to reliably predict the transverse composite response at the microscale. Furthermore, verification and validation through length-scale specific experimental techniques are necessary. It is implied through this study that testing thin laminates fabricated from a single ply eliminate more complex failure modes associated with stacked laminates such as inter-ply delamination and debonding [8], [20]. By testing a single-ply laminate, a more suitable comparison was achieved with the micromechanical model where the dominant mode of failure was matrix failure due to stress concentrations. Additionally, any potential size effect on the transverse strength was reduced by testing thin laminates at a comparable length scale. As a result, excellent agreement was observed between the virtual and physical test cases. This study also highlighted the importance of considering the effect of the manufacturing process on transverse performance. Ignoring the process-induced residual stress generation led to overestimation of the transverse composite strength which can yield inaccurate allowables during composite design. Therefore, process modeling and physical test techniques presented herein can be employed to design, test, and optimize composite microstructures and facilitate the advancement of CME

CONCLUSIONS

The prediction of transverse tensile strength of PMCs using computational micromechanics was presented in this study. A robust and reliable computational framework was presented to facilitate process modeling and virtual mechanical testing of composite microstructures. The process modeling provided a reliable estimate of the residual stress generation in composite microstructures. Virtual mechanical tests in transverse tension were performed on the processed RVEs and their transverse response predictions were compared, for the first time, to those from physical testing of thin laminates fabricated from a single carbon fiber ply. Excellent agreement was observed between the virtual and physical test results suggesting that physical testing was performed at an appropriate length scale.

There is a critical need for computational techniques such as those presented in this research. Process modeling can prove as an excellent tool for optimizing the manufacturing process to achieve the desired internal stress state for enhanced part

performance. Physics-based damage modeling and virtual mechanical testing can provide reliable estimates of composite failure and part performance. Length-scale specific physical testing can serve as a critical validation step for design certifications in addition to providing valuable insight into length-scale specific damage mechanisms that dictate composite performance. The establishment and integration of design strategies, such as those presented in this paper, into the composite design and development process are necessary to develop a unified multiscale framework for virtual composite processing and testing.

ACKNOWLEDGEMENTS

This material is based upon the work supported partially by the National Science Foundation under grant number IIP – 1362022 (Collaborative Research: IUCRC for Wind Energy, Science, Technology and Research) and the Air Force Office of Scientific Research, and the National Science Foundation under grant number IIP – 1826232. Any opinions, findings, and conclusions, or recommendations expressed in this material are those of the author(s) and do not necessarily reflect the views of the National Science Foundation. The authors would like to thank NASA for their support of this research under grant numbers 80NSSC19K1246 and NNX17AJ32G. The authors would like to acknowledge the WindSTAR Industrial Advisory Board (IAB) members Steve Nolet, Amir Salimi (TPI Composites Inc.) for their technical contributions and Paul Ubrich, Nathan Bruno, Mirna Robles (Hexion Inc.) for their technical insight into the project and providing the resin material.

REFERENCES

[1] X. Liu and W. Yu, "Multiscale Modeling of Viscoelastic Behaviors of Textile Composites Using Mechanics of Structure Genome," Kissimmee, Florida, Jan. 2018. doi: 10.2514/6.2018-0899.

[2] X. Liu, D. Furrer, J. Kosters, and H. Holmes, "Vision 2040: A Roadmap for Integrated, Multiscale Modeling and Simulation of Materials and Systems," NASA, Mar. 2018. Accessed: Mar. 03, 2020. [Online]. Available: https://ntrs.nasa.gov/search.jsp?R=20180002010

[3] J. LLorca *et al.*, "Multiscale Modeling of Composite Materials: a Roadmap Towards Virtual Testing," *Advanced Materials*, vol. 23, no. 44, pp. 5130–5147, 2011, doi: 10.1002/adma.201101683.

[4] B. Cox and Q. Yang, "In Quest of Virtual Tests for Structural Composites," *Science*, vol. 314, no. 5802, pp. 1102–1107, Nov. 2006, doi: 10.1126/science.1131624.

[5] C. He *et al.*, "A multiscale elasto-plastic damage model for the nonlinear behavior of 3D braided composites," *Composites Science and Technology*, vol. 171, pp. 21–33, Feb. 2019, doi: 10.1016/j.compscitech.2018.12.003.

[6] I. M. Gitman, H. Askes, and L. J. Sluys, "Coupled-volume multi-scale modelling of quasi-brittle material," *European Journal of Mechanics - A/Solids*, vol. 27, no. 3, pp. 302–327, May 2008, doi: 10.1016/j.euromechsol.2007.10.004.

[7] X. Hui, Y. Xu, and W. Zhang, "An integrated modeling of the curing process and transverse tensile damage of unidirectional CFRP composites," *Composite Structures*, vol. 263, p. 113681, May 2021, doi: 10.1016/j.compstruct.2021.113681.

[8] S. Kohler, J. Cugnoni, R. Amacher, and J. Botsis, "Transverse cracking in the bulk and at the free edge of thin-ply composites: Experiments and multiscale modelling," *Composites Part A: Applied Science and Manufacturing*, vol. 124, p. 105468, Sep. 2019, doi: 10.1016/j.compositesa.2019.05.036.

[9] P. Naghipour *et al.*, "Multiscale static analysis of notched and unnotched laminates using the generalized method of cells:," *Journal of Composite Materials*, Jun. 2016, doi: 10.1177/0021998316651708.

[10] V. P. Nguyen, O. Lloberas-Valls, M. Stroeven, and L. J. Sluys, "Homogenization-based multiscale crack modelling: From micro-diffusive damage to macro-cracks," *Computer Methods in Applied Mechanics and Engineering*, vol. 200, no. 9, pp. 1220–1236, Feb. 2011, doi: 10.1016/j.cma.2010.10.013.

[11] V. P. Nguyen, M. Stroeven, and L. J. Sluys, "Multiscale continuous and discontinuous modeling of heterogeneous materials: a review on recent developments," *J. Multiscale Modelling*, vol. 03, no. 04, pp. 229–270, Dec. 2011, doi: 10.1142/S1756973711000509.

[12] W. V. Liebig, C. Leopold, T. Hobbiebrunken, and B. Fiedler, "New test approach to determine the transverse tensile strength of CFRP with regard to the size effect," *Composites Communications*, vol. 1, pp. 54–59, Oct. 2016, doi: 10.1016/j.coco.2016.09.003.

[13] C. M. Arndt, N. V. de Carvalho, and M. W. Czabaj, "Experimental reexamination of transverse tensile strength for IM7/8552 tape-laminate composites," *Journal of Composite Materials*, vol. 54, no. 23, pp. 3297–3312, Sep. 2020, doi: 10.1177/0021998320914065.

[14] C. H. Mefford, Y. Qiao, and M. Salviato, "Failure behavior and scaling of graphene nanocomposites," *Composite Structures*, vol. 176, pp. 961–972, Sep. 2017, doi: 10.1016/j.compstruct.2017.06.013.

[15] T. K. Obrien and S. A. Salpekar, "Scale effects on the transverse tensile strength of graphite epoxy composites," presented at the ASTM Symposium on Composite Materials: Testing and Design, Pittsburgh, PA, Jun. 1992. Accessed: Dec. 22, 2021. [Online]. Available: https://ntrs.nasa.gov/citations/19920024460

[16] M. R. Wisnom, "Size effects in the testing of fibre-composite materials," *Composites Science and Technology*, vol. 59, no. 13, pp. 1937–1957, Oct. 1999, doi: 10.1016/S0266-3538(99)00053-6.

[17] I. De Baere, W. Van Paepegem, M. Quaresimin, and J. Degrieck, "On the tension–tension fatigue behaviour of a carbon reinforced thermoplastic part I: Limitations of the ASTM D3039/D3479 standard," *Polymer Testing*, vol. 30, no. 6, pp. 625–632, Sep. 2011, doi: 10.1016/j.polymertesting.2011.05.004.

[18] J. M. F. de Paiva, S. Mayer, and M. C. Rezende, "Comparison of tensile strength of different carbon fabric reinforced epoxy composites," *Mat. Res.*, vol. 9, pp. 83–90, Mar. 2006, doi: 10.1590/S1516-14392006000100016.

[19] R. Guo, L. Mao, Z. Xin, and L. Ding, "Experimental characterization and micro-modeling of transverse tension behavior for unidirectional glass fibre-reinforced composite," *Composites Science and Technology*, p. 109359, Feb. 2022, doi: 10.1016/j.compscitech.2022.109359.

[20] J. Galos, "Thin-ply composite laminates: a review," *Composite Structures*, vol. 236, p. 111920, Mar. 2020, doi: 10.1016/j.compstruct.2020.111920.

[21] M. Flores, A. Sharits, R. Wheeler, N. Sesar, and D. Mollenhauer, "Experimental analysis of polymer matrix composite microstructures under transverse compression loading," *Composites Part A: Applied Science and Manufacturing*, vol. 156, p. 106859, May 2022, doi: 10.1016/j.compositesa.2022.106859.

[22] S. E. Stapleton, L. Appel, J.-W. Simon, and S. Reese, "Representative volume element for parallel fiber bundles: Model and size convergence," *Composites Part A: Applied Science and Manufacturing*, vol. 87, pp. 170–185, Aug. 2016, doi: 10.1016/j.compositesa.2016.04.018.

[23] S. P. Shah and M. Maiarù, "Effect of Manufacturing on the Transverse Response of Polymer Matrix Composites," *Polymers*, vol. 13, no. 15, Art. no. 15, Jan. 2021, doi: 10.3390/polym13152491.

[24] S. P. Shah, S. U. Patil, C. J. Hansen, G. M. Odegard, and M. Maiarù, "Process modeling and characterization of thermoset composites for residual stress prediction," *null*, pp. 1–12, Dec. 2021, doi: 10.1080/15376494.2021.2017527.

[25] M. R. Kamal and S. Sourour, "Kinetics and thermal characterization of thermoset cure," *Polymer Engineering & Science*, vol. 13, no. 1, pp. 59–64, 1973, doi: https://doi.org/10.1002/pen.760130110.

[26] Z. P. Bažant and B. H. Oh, "Crack band theory for fracture of concrete," *Mat. Constr.*, vol. 16, no. 3, pp. 155–177, May 1983, doi: 10.1007/BF02486267.

[27] E. J. Pineda, B. A. Bednarcyk, A. M. Waas, and S. M. Arnold, "Progressive failure of a unidirectional fiber-reinforced composite using the method of cells: Discretization objective computational results," *International Journal of Solids and Structures*, vol. 50, no. 9, pp. 1203–1216, May 2013, doi: 10.1016/j.ijsolstr.2012.12.003.

[28] D30 Committee, "ASTM D3039-17: Standard Test Method for Tensile Properties of Polymer Matrix Composite Materials," ASTM International. doi: 10.1520/D3039_D3039M-17.

[29] D20 Committee, "ASTM D792-20: Standard Test Methods for Density of Specific Gravity (Relative Density) of Plastics by Displacements," ASTM International. doi: 10.1520/D0792-20.

[30] E37 Committee, "ASTM E1131-20: Standard Test Method for Compositional Analysis by Thermogravimetry," ASTM International. doi: 10.1520/E1131-20.

[31] J. Blaber, B. Adair, and A. Antoniou, "Ncorr: Open-Source 2D Digital Image Correlation Matlab Software," *Exp Mech*, vol. 55, no. 6, pp. 1105–1122, Jul. 2015, doi: 10.1007/s11340-015-0009-1.

[32] R. Harilal and M. Ramji, "Adaptation of Open Source 2D DIC Software Ncorr for Solid Mechanics Applications," presented at the 9th International Symposium on Advanced Science and Technology in Experimental Mechanics, New Delhi, India, Jul. 2015. Accessed: May 23, 2022. [Online]. Available: https://doi.org/10.1007/s11340-015-0009-1

[33] J. D. Littell, C. R. Ruggeri, R. K. Goldberg, G. D. Roberts, W. A. Arnold, and W. K. Binienda, "Measurement of Epoxy Resin Tension, Compression, and Shear Stress–Strain Curves over a Wide Range of Strain Rates Using Small Test Specimens," *Journal of Aerospace Engineering*, vol. 21, no. 3, pp. 162–173, Jul. 2008, doi: 10.1061/(ASCE)0893-1321(2008)21:3(162).